

# Photoproduction of the $f_2(1270)$ resonance

Ju-Jun Xie<sup>1,2,3,\*</sup> and E. Oset<sup>1,4,†</sup>

<sup>1</sup>*Institute of Modern Physics, Chinese Academy of Sciences, Lanzhou 730000, China*

<sup>2</sup>*Research Center for Hadron and CSR Physics, Institute of Modern Physics of CAS and Lanzhou University, Lanzhou 730000, China*

<sup>3</sup>*State Key Laboratory of Theoretical Physics, Institute of Theoretical Physics, Chinese Academy of Sciences, Beijing 100190, China*

<sup>4</sup>*Departamento de Física Teórica and IFIC, Centro Mixto Universidad de Valencia-CSIC Institutos de Investigación de Paterna, Aptdo. 22085, 46071 Valencia, Spain*

(Dated: November 23, 2015)

We have performed a calculation of the  $\gamma p \rightarrow \pi^+\pi^-p$  reaction, where the two pions have been separated in  $D$ -wave producing the  $f_2(1270)$  resonance. We use elements of the local hidden gauge approach that provides the interaction of vector mesons in which the  $f_2(1270)$  resonance appears as a  $\rho$ - $\rho$  molecular state in  $L = 0$  and spin 2. The vector meson dominance, incorporated in the local hidden gauge approach converts a photon into a  $\rho^0$  meson and the other meson connects the photon with the proton. The picture is simple and has no free parameters, since the parameters of the theory have been constrained in the previous study of the vector-vector states. In a second step we introduce new elements, not present in the local hidden gauge approach, adapting the  $\rho$  propagator to Regge phenomenology and introducing the  $\rho NN$  tensor coupling. We find that both the differential cross section as well as the  $t$  dependence of the cross section are in good agreement with the experimental results and provide support for the molecular picture of the  $f_2(1270)$  in the first baryonic reaction where it has been tested.

PACS numbers: 13.60.Le, 13.75.Lb, 14.40.Cs

## I. INTRODUCTION

The  $f_2(1270)$  is a resonance that plays a prominent role in many reactions. For instance in  $\pi^0\pi^0 \rightarrow \gamma\gamma$  it shows with a strength much bigger than the corresponding one of the  $f_0(980)$  [1, 2]. From the theoretical point of view, the  $f_2(1270)$  resonance has been widely accepted as an ordinary  $q\bar{q}$  state belonging to a  $P$ -wave nonet of tensor mesons [3, 4]. However, this wisdom was challenged by the work of Ref. [5] where the interaction of vector mesons was studied and the  $f_2(1270)$  emerged as one of the dynamically generated states from the  $\rho$ - $\rho$  interaction. The vector-vector interaction is described by means of the local hidden gauge Lagrangians [6–9] and the unitarization of this interaction leads to vector-vector scattering amplitudes that show poles for some states of spin  $J = 0, 1, 2$  in  $L = 0$ . One of them is the  $f_2(1270)$ . The generalization to  $SU(3)$  of the  $\rho$ - $\rho$  interaction was done following the same lines but with coupled channels [10] and the  $f_2(1270)$  appeared as a dynamically generated state of the  $\rho$ - $\rho$  interaction with parallel spins, corroborating the findings of Ref. [5]. The reason for the large binding of the  $f_2(1270)$  is a very large interaction of the  $\rho$ - $\rho$  in  $J = 2$ , much larger than for other channels, and larger than other interactions known in hadron physics.

The molecular nature of  $f_2(1270)$  claimed in Refs. [5,

10] has been successfully tested in a large number of processes. In Ref. [11] it was shown that it leads to a very good description of the decay rate for  $f_2(1270) \rightarrow \gamma\gamma$ . It was also shown in Ref. [12] that the decay rates for two photons and one photon-one vector decays of the  $f_0(1370)$ ,  $f_2(1270)$ ,  $f_0(1710)$ ,  $f_2'(1525)$  and  $K_2^*(1430)$  were in good agreement with available data. A study of the  $J/\psi \rightarrow \phi(\omega)f_2(1270)$ ,  $f_2'(1525)$  and  $J/\psi \rightarrow K^{*0}(892)\bar{K}_2^{*0}(1430)$  decays was also done within this picture in Ref. [13] and good results were obtained. Another test conducted along these lines was the radiative decay of  $J/\psi$  into  $f_2(1270)$ ,  $f_2'(1525)$ ,  $f_0(1370)$  and  $f_0(1710)$  which was done in Ref. [14] and good results were obtained compared with the available experimental information. Similarly, predictions for  $\psi(2S)$  decay into  $\omega(\phi)f_2(1270)$ ,  $\omega(\phi)f_2'(1525)$ ,  $K^{*0}(892)\bar{K}_2^{*0}(1430)$  and radiative decay of  $\Upsilon(1S)$ ,  $\Upsilon(2S)$ ,  $\psi(2S)$  into  $\gamma f_2(1270)$ ,  $\gamma f_2'(1525)$ ,  $\gamma f_0(1370)$ ,  $\gamma f_0(1710)$  were done in Refs. [15, 16] with also good agreement with available experiments. More recently it was shown in Ref. [17] that the ratio of the decay widths of  $\bar{B}_s^0 \rightarrow J/\psi f_2(1270)$  to  $\bar{B}_s^0 \rightarrow J/\psi f_2'(1525)$  is compatible with the experimental values of [18]. The nature of these states as vector meson-vector meson composite states has undergone a large number of test than any other model. Yet, all the test have been done in the mesonic sector and not in the baryonic sector. The recent measurement of the photoproduction of  $f_2(1270)$  in Jefferson Lab [19] offers us the first opportunity to do this new test, which we conduct here.

On the theoretical side there is a study of this reaction in Ref. [20], where the idea is to create the  $f_2(1270)$  as the final state interaction of two pions in  $D$ -wave. Hence, one constructs a mechanism for two pion production and

\*Electronic address: xiejujun@impcas.ac.cn

†Electronic address: oset@ific.uv.es

then lets the pions interact in  $D$ -wave to produce the  $f_2(1270)$  resonance. Our picture has some similarity with this idea in the sense that we also generate the resonance from the final state interaction of two mesons, but these two mesons are two  $\rho$  instead of two pions. Hence, the mechanism consists on the production of two  $\rho$ , for which vector meson dominance is used, and then the two  $\rho$  mesons, upon interaction, produce the  $f_2(1270)$ . Dealing with baryons at a relatively large energy and large momentum transfers, we have to introduce some elements of Regge phenomenology and consider the  $\rho NN$  tensor coupling, in addition to the vector coupling which stems from chiral dynamics. The results obtained are in good agreement with experiment, both for the invariant mass dependence and the  $t$  dependence, offering new support for the picture of the  $f_2(1270)$  as a  $\rho$ - $\rho$  molecular state.

The present paper is organized as follows. In Sec. II we discuss the formalism and the main ingredients of the model. In Sec. III, we present our main results and finally, a short summary and conclusions are given in Sec. IV.

## II. FORMALISM AND INGREDIENTS

### A. Feynman amplitudes

In Ref. [5] the  $\rho$ - $\rho$  amplitudes in  $L = 0$  were classified in terms of the spin of the system, which was produced by the  $\rho$  polarization. Spin-projector operators were written in terms of the  $\rho$  polarization vectors and concretely, for spin  $S = 2$ , the projector was given by

$$P^{(2)} = \left[ \frac{1}{2}(\epsilon_i^{(1)}\epsilon_j^{(2)} + \epsilon_j^{(1)}\epsilon_i^{(2)}) - \frac{1}{3}\epsilon_i^{(1)}\epsilon_l^{(2)}\delta_{ij} \right] \times \left[ \frac{1}{2}(\epsilon_i^{(3)}\epsilon_j^{(4)} + \epsilon_j^{(3)}\epsilon_i^{(4)}) - \frac{1}{3}\epsilon_m^{(3)}\epsilon_m^{(4)}\delta_{ij} \right],$$

where  $\epsilon_i^{(k)}$  are the three spatial components ( $i$ ) vector polarization of the  $\rho$  meson  $k$ , in the order of  $\rho(2) \rightarrow \rho(3) + \rho(4)$ . The momenta of the external mesons is assumed to be small with respect to that of the  $\rho$ , such that the time component of the polarization is neglected. This is the case of the polarization of photons, where we only have transverse components. This was also discussed in Ref. [21] that extra terms like the momentum of the particles were small in this process, justifying the success of the radiative decays despite of the photons not having small momenta.

As we can see, the  $P^{(2)}$  projector is factorized in blocks corresponding to the initial vectors and another corresponding to the final vectors. The amplitude

to a pole that represents a resonance is then written as

$$t_{\text{pole}} \simeq \frac{g_T^2 P_{\text{initial}}^{(2)} P_{\text{final}}^{(2)}}{s - s_R}, \quad (2)$$

$$P_{\text{initial}}^{(2)} = \frac{1}{2}(\epsilon_i^{(1)}\epsilon_j^{(2)} + \epsilon_j^{(1)}\epsilon_i^{(2)}) - \frac{1}{3}\epsilon_l^{(1)}\epsilon_l^{(2)}\delta_{ij}, \quad (3)$$

$$P_{\text{final}}^{(2)} = \frac{1}{2}(\epsilon_i^{(3)}\epsilon_j^{(4)} + \epsilon_j^{(3)}\epsilon_i^{(4)}) - \frac{1}{3}\epsilon_m^{(3)}\epsilon_m^{(4)}\delta_{ij}, \quad (4)$$

where  $s_R$  is the pole position and  $g_T$  the coupling of the resonance to the  $\rho\rho$  component in isospin  $I = 0$  and spin  $S = 2$ . Eq. (2) is the representation of a resonance amplitude, for instance the  $f_2(1270)$  in the present case, as shown in Fig. 1 (a).

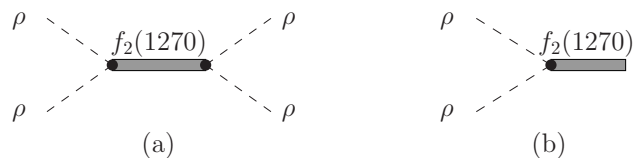


FIG. 1: (a): The  $\rho\rho$  amplitude dominated by the  $f_2(1270)$  pole; (b): Representation of the  $f_2(1270)$  coupling to  $\rho\rho$ .

Then the coupling of a resonance to  $\rho\rho$  is given by the diagram of Fig. 1 (b), and is expressed in terms of the vertex [11]

$$t_{R \rightarrow \rho\rho} = g_T P_{\text{initial}}^{(2)}, \quad (5)$$

with  $g_T^2 = 150 \text{ GeV}^2$  that was evaluated in Ref. [11] from the  $\rho\rho$  amplitude generated in Ref. [5].

From the perspective that the  $f_2(1270)$  is generated from the  $\rho\rho$  interaction, the picture for  $f_2(1270)$  photo-production proceeds via the creation of two  $\rho$  mesons by the  $\gamma p$  initial state in a primary step and the interaction of the two  $\rho$  mesons generating the resonance. Alternatively we can think that the resonance couples to two  $\rho$  mesons, as depicted in Fig. 1 (b) and there two  $\rho$  mesons couple to the  $\gamma p$  system. This mechanism is expressed by the Feynman diagram of Fig. 2.

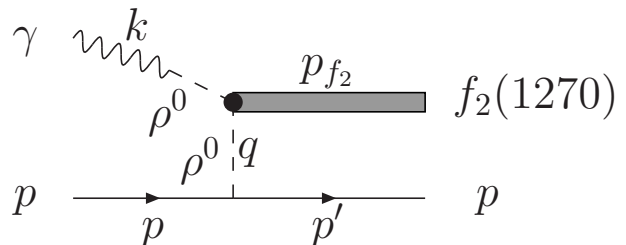


FIG. 2: Diagrammatic representation of the  $f_2(1270)$  photo-production. We also show the definition of the kinematical variables ( $k, p, p', q, p_{f_2}$ ) that we used in the present calculation. In addition, we use  $q = p' - p$ .

As we see, the photon gets converted into one  $\rho^0$ , a characteristic of the local hidden gauge Lagrangian, and

the other  $\rho^0$  becomes a virtual  $\rho$  connecting to the proton. Apart from the vertex of Eq. (5), we need now two ingredients, the  $\gamma$ - $\rho^0$  conversion vertex and the  $\rho NN$  vertex. The  $\gamma$ - $\rho^0$  conversion vertex is easily obtained from the local hidden gauge Lagrangian [6–9] (see Ref. [22] for a practical set of rules) and we have [11]

$$-it_{\rho^0\gamma} = \frac{-i}{\sqrt{2}} \frac{eM_\rho^2}{g} \epsilon_\mu(\rho) \epsilon^\mu(\gamma), \quad (6)$$

with

$$g = \frac{M_\rho}{2f}; \quad f = 93 \text{ MeV}; \quad \frac{e^2}{4\pi} = \frac{1}{137}. \quad (7)$$

The  $\rho^0$  polarization of Eq. (6) is contracted with the one of the  $\rho$  in the vertex of Eq. (5) and the polarization vector of the  $\rho$  in Eq. (5) gets converted into the one of the photon. The other ingredient that we need is the vector-nucleon-nucleon vertex, which is given by the Lagrangian

$$\mathcal{L}_{BBV} = g(\langle \bar{B}\gamma^\mu[V_\mu, B] \rangle + \langle \bar{B}\gamma^\mu B \rangle \langle V_\mu \rangle), \quad (8)$$

which provides a  $\rho^0 pp$  vertex

$$-it_{\rho^0 pp} = i \frac{g}{\sqrt{2}} \bar{p} \gamma^\mu p \epsilon_\mu(\rho^0). \quad (9)$$

On the other hand, there are generally two types of strong couplings, vector and tensor couplings, for the  $\rho NN$  vertex, which is given in terms of the interaction Lagrangian density by

$$\mathcal{L}_{\rho NN} = -g_{\rho NN} \bar{N}(\gamma^\mu - \frac{\kappa_\rho}{2m_N} \sigma^{\mu\nu} \partial_\nu) \vec{\tau} \cdot \vec{\rho}_\mu N, \quad (10)$$

which gives a  $\rho^0 pp$  vertex

$$-it_{\rho^0 pp} = ig_{\rho NN} \bar{p}(\gamma^\mu + \frac{i\kappa_\rho}{2m_N} \sigma^{\mu\nu} q_\nu) p \epsilon_\mu(\rho^0), \quad (11)$$

with  $g_{\rho NN}^2/4\pi = 0.9$  and  $\kappa_\rho = 6.1$  obtained from the Bonn potential [23]. The tensor  $\rho NN$  coupling is important in describing the  $\Delta^*(1620)$  and  $N^*(1535)$  production in the  $\pi N$  and  $NN$  collisions [24–27]. Thus, we will also check its contribution in the present process. Note that  $g/\sqrt{2}$  from the local hidden gauge approach is 2.93, while the equivalent quantity  $g_{\rho NN}$  of Eq. (11) is 3.36. They differ in 12%. When including the tensor coupling we shall use the  $g_{\rho NN}$  coupling of the Bonn potential [23].

There is one more consideration to make. The amplitude of Eq. (2) is evaluated for a  $\rho\rho$  state in the unitary normalization, which for  $I = 0$  is given by (recall  $|\rho^+ \rangle = -|11 \rangle$ )

$$|\rho\rho, I = 0 \rangle = -\frac{1}{\sqrt{6}}(\rho^+ \rho^- + \rho^- \rho^+ + \rho^0 \rho^0). \quad (12)$$

This has a factor  $\frac{1}{\sqrt{2}}$  extra with respect to the good normalization and is taken to account for the identity of the particles in the intermediate states. The good amplitude

will have  $g_T$  of Eqs. (2) and (5) multiplied by  $\sqrt{2}$ . In addition, in order to project over  $\rho^0 \rho^0$  we must multiply the coupling to the  $I = 0$  state by  $\frac{1}{\sqrt{3}}$ . Altogether, the coupling  $\tilde{g}_T$  to be used for  $\rho^0 \rho^0$  is <sup>1</sup>

$$\tilde{g}_T = -\sqrt{\frac{2}{3}} g_T. \quad (13)$$

When considering photonuclear processes gauge invariance of the amplitude is an important test, although it often happens that terms that are relevant in the test of gauge invariance are small or negligible in the physical amplitudes [28, 29]. Yet, in the present case, a thorough test of gauge invariance was conducted in Ref. [22] for the radiative decay of axial vector mesons within the local hidden gauge approach, and in particular in Ref. [11] for the amplitude  $\rho\rho \rightarrow \rho\gamma$ , which is the one we have here, with the two  $\rho$  mesons merging later on the  $f_2(1270)$  state. The test involves terms of  $\rho$  exchange in the  $\rho\rho$  interaction and four body contact terms, but all these ingredients are finally included in the effective coupling of the  $f_2(1270)$  resonance to the two  $\rho$  mesons.

Considering the vertices described above, the  $T$  matrix for the diagram of Fig. 2 is given in the case of  $\rho NN$  vector coupling by

$$\begin{aligned} -iT_{\gamma p \rightarrow f_2(1270)p} &= -i \frac{e\tilde{g}_T}{2} \left\{ \frac{1}{2} [\epsilon_i(\gamma) \epsilon_j(\rho) + \epsilon_j(\gamma) \epsilon_i(\rho)] \right. \\ &\quad \left. - \frac{1}{3} \epsilon_m(\gamma) \epsilon_m(\rho) \delta_{ij} \right\} \frac{1}{q^2 - M_\rho^2} \langle M' | \gamma^\mu \epsilon_\mu(\rho) | M \rangle, \quad (14) \end{aligned}$$

with  $M$  and  $M'$  the spin third component of the initial and final proton. We must perform the sum over the polarizations of the  $\rho$  meson exchanged in Fig. 2 and then we get

$$\begin{aligned} T_{\gamma p \rightarrow f_2(1270)p} &= \frac{e\tilde{g}_T}{2} \frac{1}{q^2 - M_\rho^2} \left[ \frac{1}{2} \epsilon_i(\gamma) (-g_{j\mu} + \frac{q_j q_\mu}{M_\rho^2}) \right. \\ &\quad \left. + \frac{1}{2} \epsilon_j(\gamma) (-g_{i\mu} + \frac{q_i q_\mu}{M_\rho^2}) - \frac{1}{3} \epsilon_m(\gamma) \delta_{ij} (-g_{m\mu} + \frac{q_m q_\mu}{M_\rho^2}) \right] \\ &\quad \langle M' | \gamma^\mu | M \rangle. \quad (15) \end{aligned}$$

In Eqs. (14) and (15) all the components in  $g_{i\mu}$ , etc,  $q_i$ ,  $q_j$ ,  $q_\mu$  are covariant. The latin indices run over 1, 2, 3 and the  $\mu$  index from 0, 1, 2, 3.

In order to calculate  $\sum \sum |T|^2$  when we include the

<sup>1</sup> In Ref. [11] the  $\sqrt{2}$  factor is not implemented because it is compensated by not dividing by two the integrated width, as it corresponds to two final identical particles (two photons).

$\rho NN$  tensor coupling, we calculate

$$\begin{aligned}
& \frac{1}{2} \sum_{M', M} \langle M' | \Gamma^\mu | M \rangle \langle M | (\Gamma^{\mu'})^\dagger | M' \rangle \\
&= \frac{1}{2} \sum_{r, r'} \bar{u}_{r'}(p') \Gamma^\mu u_r(p) \bar{u}_r(p) \Gamma^{\mu'} u_{r'}(p') \\
&= \frac{1}{2} \text{Tr} \left[ \frac{\not{p}' + m_p}{2m_p} \Gamma^\mu \frac{\not{p} + m_p}{2m_p} \Gamma^{\mu'} \right] \\
&= \frac{1}{8m_p^2} \text{Tr} [(\not{p}' + m_p) \Gamma^\mu (\not{p} + m_p) \Gamma^{\mu'}], \quad (16)
\end{aligned}$$

where  $\Gamma^\mu = \gamma^\mu$  or  $\gamma^\mu + \frac{i\kappa_\rho}{2m_N} \sigma^{\mu\nu} q_\nu$  for  $\rho NN$  only vector coupling or full vector and tensor couplings, respectively. Hence, we have

$$\begin{aligned}
\bar{\sum} \sum |T|^2 &= \frac{e^2 \tilde{g}_T^2}{32m_p^2 (q^2 - M_\rho^2)^2} \sum_{\gamma \text{ pol.}} \sum_{i, j, m, l} \sum_{\mu, \mu'} \\
& \left[ \frac{1}{2} \epsilon_i(\gamma) (-g_{j\mu} + \frac{q_j q_\mu}{M_\rho^2}) + \frac{1}{2} \epsilon_j(\gamma) (-g_{i\mu} + \frac{q_i q_\mu}{M_\rho^2}) \right. \\
& - \frac{1}{3} \epsilon_m(\gamma) \delta_{ij} (-g_{m\mu} + \frac{q_m q_\mu}{M_\rho^2}) \left. \right] \left[ \frac{1}{2} \epsilon_i(\gamma) (-g_{j\mu'} + \frac{q_j q_{\mu'}}{M_\rho^2}) \right. \\
& + \frac{1}{2} \epsilon_j(\gamma) (-g_{i\mu'} + \frac{q_i q_{\mu'}}{M_\rho^2}) - \frac{1}{3} \epsilon_l(\gamma) \delta_{ij} (-g_{l\mu'} + \frac{q_l q_{\mu'}}{M_\rho^2}) \left. \right] \\
& \text{Tr} [(\not{p}' + m_p) \Gamma^\mu (\not{p} + m_p) \Gamma^{\mu'}], \quad (17)
\end{aligned}$$

and we sum explicitly over all the indices and the two photon polarization which we write explicitly as

$$\epsilon^{(1)}(\gamma) = \begin{pmatrix} 1 \\ 0 \\ 0 \end{pmatrix}; \quad \epsilon^{(2)}(\gamma) = \begin{pmatrix} 0 \\ 1 \\ 0 \end{pmatrix}, \quad (18)$$

where we have assumed that the photon travels in the direction.

### B. Regge contributions

In this section we explain how the Regge contributions are implemented. We base our model on the exchange of a dominant  $\rho$ -Regge trajectory, as suggested in Refs. [33–34]. The  $\rho$  trajectory represents the exchange of a family of particles with  $\rho$ -type internal quantum numbers. In order to take the Regge contribution into account, we replace the normal  $\rho$  meson Feynman propagator by so-called Regge propagator, while keeping the rest of

vertex structure, i.e. <sup>2</sup>

$$\begin{aligned}
& \frac{1}{q^2 - m_\rho^2} \quad (\text{normal}) \\
& \rightarrow \hat{f} \left( \frac{s}{s_0} \right)^{\alpha_\rho(t)-1} \Gamma(1 - \alpha_\rho(t)) \quad (\text{Regge}), \quad (19) \\
& \alpha_\rho(t) = 0.55 + 0.8t, \quad (20)
\end{aligned}$$

with  $s_0 = 1 \text{ GeV}^2$  and  $\hat{f}$  a overall normalization factor of the Reggeon exchange contribution. This undetermined scale will be fitted to the available data.

Note that the Regge propagator of Eq. (19) has the property that it reduces to the Feynman propagator  $1/(q^2 - m_\rho^2)$  if one approaches the first pole on the trajectory (i.e.,  $q^2 \rightarrow m_\rho^2$ ). This means that the farther we go from the pole, the more the result of the Regge model will differ from conventional Feynman-diagram-based models.

### C. Differential cross section

If we consider the  $f_2(1270)$  as an elementary particle, we find

$$\frac{d\sigma}{d\Omega} = \frac{m_p^2}{16\pi^2 s} \frac{|\vec{p}_{f_2}|}{|k|} \bar{\sum} \sum |T|^2, \quad (21)$$

where  $\vec{p}_{f_2}$  and  $\vec{k}$  are the three momenta of final  $f_2(1270)$  and initial photon in the center of mass frame (c.m.), and taking into account that  $t = q^2 = (p - p')^2 = 2m_p^2 - 2E(p)E(p') + 2\vec{p} \cdot \vec{p}'$ , we get

$$\frac{d\sigma}{dt} = \frac{m_p^2}{16\pi s |k|^2} \bar{\sum} \sum |T|^2. \quad (22)$$

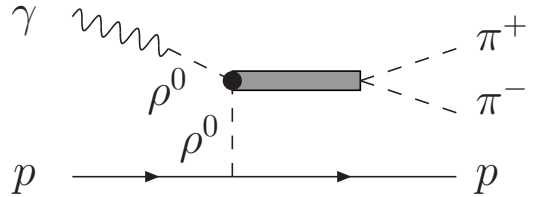


FIG. 3: Feynman diagram for the  $\gamma p \rightarrow p \pi^+ \pi^-$  reaction.

The Eq. (22) can be generalized for the case when the  $f_2(1270)$  is explicitly allowed to decay into two pions as

<sup>2</sup> In Refs. [30–34], trajectories with a rotating ( $e^{-i\pi\alpha_\rho(t)}$ ) phase, instead of a constant phase were assumed. This phase factor only affects the interference between different Regge contributions, which is not the case of the present calculation. Besides, another phase factor,  $(-1 + e^{-i\pi\alpha_\rho(t)})/2$ , was used in Ref. [35]. This later phase factor will give a dip around  $t \sim -0.7 \text{ GeV}^2$  (corresponding to  $\alpha_\rho(t) = 0$ ). Nevertheless, we will see that the CLAS data favor a constant phase as used in Eq. (19).

shown in Fig. 3 by working out the three body phase space and we find

$$\frac{d^2\sigma}{dM_{\text{inv}}dt} = \frac{m_p^2}{8\pi^2 s |\vec{k}|^2} \frac{M_{\text{inv}}^2 \Gamma_\pi}{|M_{\text{inv}}^2 - M_{f_2}^2 + iM_{\text{inv}}\Gamma_{f_2}|^2} \times \sum \sum |T|^2, \quad (23)$$

where  $M_{\text{inv}}$  is the invariant mass distribution of the two pions,  $\Gamma_{f_2}$  is the total decay width of the  $f_2(1270)$  and  $\Gamma_\pi$  is the partial decay width of the  $f_2(1270)$  into the  $\pi\pi$  system, in our case  $\pi^+\pi^-$ . The  $\pi^+\pi^-$  decay accounts for  $\frac{2}{3}$  of the  $\pi\pi$  decay width of the  $f_2(1270)$  which is 85% of  $\Gamma_{f_2}$ . Since the  $\pi\pi$  decay is in  $D$ -wave, in order to have  $\Gamma_\pi$  and  $\Gamma_{f_2}$  in the range of invariant masses that we consider (close to the  $f_2(1270)$  resonance), we take

$$\Gamma_\pi(M_{\text{inv}}) = \Gamma_\pi^{\text{on}} \left(\frac{\tilde{q}}{q}\right)^5 \frac{M_{f_2}^2}{M_{\text{inv}}^2}, \quad (24)$$

$$\Gamma_{f_2}(M_{\text{inv}}) = 0.85\Gamma_{f_2}^{\text{on}} \left(\frac{\tilde{q}}{q}\right)^5 \frac{M_{f_2}^2}{M_{\text{inv}}^2} + 0.15\Gamma_{f_2}^{\text{on}}, \quad (25)$$

with  $\Gamma_{f_2}^{\text{on}} = 185$  MeV,  $\Gamma_\pi^{\text{on}} = 105$  MeV, and  $M_{f_2} = 1275$  MeV [36]. And

$$\tilde{q} = \frac{\lambda^{1/2}(M_{\text{inv}}^2, m_\pi^2, m_\pi^2)}{2M_{\text{inv}}}, \quad (26)$$

$$\bar{q} = \frac{\lambda^{1/2}(M_{f_2}^2, m_\pi^2, m_\pi^2)}{2M_{f_2}}, \quad (27)$$

where  $\lambda$  is the Källén function with  $\lambda(x, y, z) = (x - y - z)^2 - 4yz$ .

This kind of parametrization of the width of a resonance is common and it is meant to take into account the phase space of each decay mode as a function of the energy [10, 37, 38]. In the present case we take explicitly the phase space for the  $D$ -wave decay of the  $f_2(1270)$  into two pions, and for the rest of the width, which accounts for only 15% of the width, coming mostly from four pion decay, we have made an approximation and maintained it constant.

#### D. Background

As in Ref. [19], we consider an incoherent background contribution to the di-pion mass spectrum of the  $\gamma p \rightarrow p\pi^+\pi^-$  reaction as <sup>3</sup>

$$\frac{d^2\sigma}{dM_{\text{inv}}dt} = \frac{Cm_p^2}{2^8\pi^3 s |\vec{k}|^2} \tilde{q}, \quad (28)$$

where  $C$  is constant.

<sup>3</sup> In general, the di-pion mass distribution of  $\gamma p \rightarrow p\pi^+\pi^-$  reaction can be obtained by working out the three body phase space,  $\frac{d^2\sigma}{dM_{\text{inv}}dt} = \frac{m_p^2}{2^8\pi^3 s |\vec{k}|^2} \sum |\mathcal{M}|^2 \tilde{q}$ , with  $\mathcal{M}$  the scattering amplitude of the  $\gamma p \rightarrow p\pi^+\pi^-$  reaction.

### III. NUMERICAL RESULTS

Here we present our numerical results. First, we label three models in Table I. Model A represents our calculation including only the vector  $\rho NN$  coupling with the normal  $\rho$  meson propagator. Model B includes the vector and tensor  $\rho NN$  couplings with the normal  $\rho$  meson propagator. Model C represents the calculation including the vector and tensor  $\rho NN$  couplings with the  $\rho$ -Regge propagator.

TABLE I: Relevant combinations in Models A, B and C.

	$\rho NN$ vertex	$\rho$ propagator
Model A	vector	normal
Model B	vector + tensor	normal
Model C	vector + tensor	Regge

In Ref. [19] the  $\gamma p \rightarrow \pi^+\pi^-p$  reaction was studied in the photon energy range 3.0 – 3.8 GeV. The magnitude  $\frac{d\sigma}{dM_{\text{inv}}d\Omega_\pi dt}$  was measured, where  $M_{\text{inv}}$  is the invariant mass of the two pions,  $t$  the momentum transfer squared and  $\Omega_\pi$ , the angle of one pion measured in the  $\pi^+\pi^-$  helicity rest frame. This multiple differential cross section was then projected over the appropriate partial waves with the integral over the corresponding spherical-harmonic functions. After correcting for detector acceptance and detector efficiency,  $\frac{d\sigma}{dM_{\text{inv}}dt}$  for the corresponding partial waves was produced, such that a direct comparison with a theoretical models can be done. The projection over  $\pi^+\pi^-$   $D$ -wave was done and a neat peak around 1270 MeV, corresponding to the  $f_2(1270)$  resonance, was found (see Fig. 4) for a certain cut of the photon energy and the variable  $t$ .

Simultaneously, a photon energy averaged cross section  $\frac{d\sigma}{dt}$  was determined by considering a wide range of energies and integrating  $\frac{d\sigma}{dM_{\text{inv}}dt}$  over  $M_{\text{inv}}$  around the resonance peak. These are magnitudes that we can easily address with our theoretical framework and we show below the results obtained.

In Fig. 4 we shown the results of Models A, B and C for  $\frac{d\sigma}{dM_{\text{inv}}dt}$  as a function of  $M_{\text{inv}}$  for  $E_\gamma = 3.3$  GeV and  $t = -0.55$  GeV<sup>2</sup>, which we compare with the results of Ref. [19] measured in the range  $3.2 < E_\gamma < 3.4$  GeV,  $-0.6 < t < -0.5$  GeV<sup>2</sup>. The result shown in Fig. 4 of Model C is obtained with  $\hat{f} = 1.43$ , while for the case of Model B, we need a dipole form factor  $(\frac{\Lambda^2}{\Lambda^2 - q^2})^2$  for the  $\rho NN$  vertex to suppress the contribution of high momenta. The result shown in Fig. 4 of Model B is obtained with  $\Lambda = 0.75$  GeV. For Model A, all the parameters were determined before as discussed in previous section. Besides, in Fig. 4 we also show the results for the background with the dash-dotted line. As stated in Ref. [19], a smooth background is considered in the analysis which is introduced by the reflection of baryon resonances and

is expected to be smooth and structureless, contributing to all partial waves. We show in Fig. 4 that a smooth background that we consider of  $S$ -wave for simplicity, meant to account for the lower side of invariant masses where our model lacks some strength, would improve the agreement with the data. We do not elaborate further since this contribution is small compared to the signal of the resonance in the region of the peak.

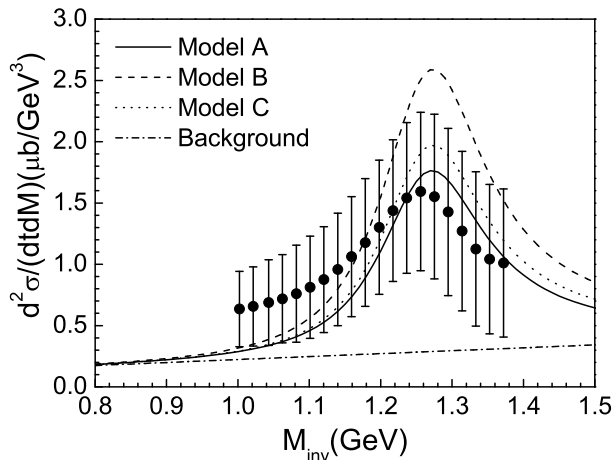


FIG. 4: Theoretical prediction for  $D$ -wave  $\pi\pi$  mass distribution at  $E_\gamma = 3.3$  GeV and  $t = -0.55$  GeV<sup>2</sup> compared with the CLAS data taken from Ref. [19]. Models A, B and C are explained in the text.

As we can see, the experimental data have a wide band of allowed values, but our theoretical results of all three models around the peak go through the middle of the band. Discrepancies below the resonance peak can be attributed to background which we have not considered in our approach, since only the resonance contribution is taken into account.

Further information can be obtained from the  $t$  dependence of the cross section. In Ref. [19] one finds  $\frac{d\sigma}{dt}$  as a function of  $t$ , obtained by integrating  $M_{\text{inv}}$  in the range  $1.275 \pm 0.185$  GeV and for photon energy in the range  $E_\gamma = 3.0 - 3.8$  GeV. We perform the calculation for this observable and the results are shown in Fig. 5. Once again, all the three models give good agreements with experiment.

Although the data seem to imply a slightly bigger slope than provided by the Model A which only the vector  $\rho NN$  coupling is included, the fact is that the results, with no free parameters, agree well with the data within errors. It seems clear that the slope provided by the  $\rho$  meson propagator in Model A accounts for the bulk of the  $t$  dependence of the cross section, but one cannot exclude extra elements to the theory that gradually change the cross section at larger values of  $t$ , too large to be accommodated within an effective theory as we have used. The Model C including both vector and tensor  $\rho NN$  cou-

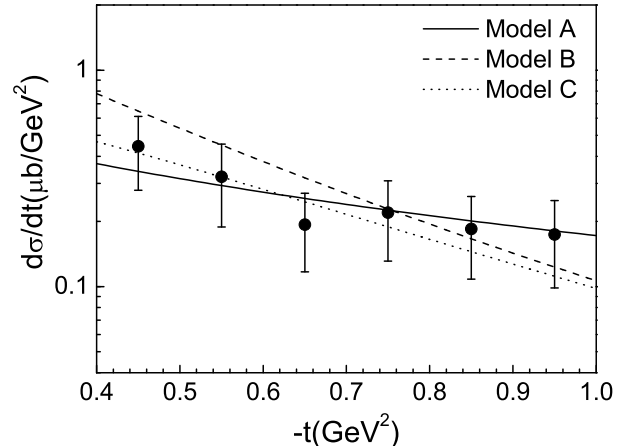


FIG. 5: Differential cross section  $\frac{d\sigma}{dt}$  as a function of  $t$ . The experimental data are taken from Ref. [19]. The small background of Fig. 4 is not considered.

plings with the  $\rho$ -Regge propagator gives similar results with Model A. Yet, for the range of energies and momentum transfers measured, it looks clear that Model A provides the basic features of the experiment and globally we can claim a good agreement with experiment.

In addition to the differential cross section, we calculate also the total cross section for the  $\gamma p \rightarrow p f_2(1270)$  reaction as a function of the photon beam energy  $E_\gamma$ . The theoretical results are shown in Fig. 6. We see that there is a clear bump structure around  $E_\gamma = 2.4$  GeV for Model C, while for Model B, this bump structure is much weaker than Model C, but stronger than Model A. Therefore, this observable, the total cross section of the  $\gamma p \rightarrow p f_2(1270)$  reaction can be employed, in the future experiments at CLAS, to test our model calculation.

#### IV. CONCLUSIONS

In this paper we have studied the  $\gamma p \rightarrow \pi^+ \pi^- p$  reaction performed in Jefferson Lab, where the two pions have been separated in  $D$ -wave, producing the  $f_2(1270)$  resonance. This resonance has been much studied recently from the point of view of a  $\rho\rho$  molecule and has passed all tests in the reactions where it has been studied. Yet, all the reactions were mesonic reactions. This is the first time where this idea has been tested in a baryonic reaction. The elements needed for the test are very simple, which offers a special transparency in the interpretation of the results. On the one side the  $f_2(1270)$  couples to  $\rho\rho$  in  $I = 0$  and the value of the coupling has been obtained before in the theory that provides the  $f_2(1270)$  as a  $\rho\rho$  molecule based on the local hidden gauge formalism for the interaction of vector mesons. With this coupling and the vector meson dominance hypothesis, incorporated in

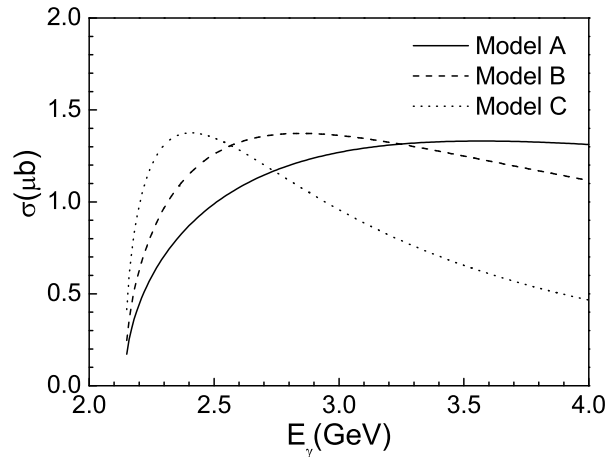


FIG. 6: Total cross section for the  $\gamma p \rightarrow p f_2(1270)$  reaction as a function of  $E_\gamma$ . The small background of Fig. 4 is not considered.

the local hidden gauge approach, the photon gets converted into one of the  $\rho^0$  of the  $\rho\rho$  formation state of the  $f_2(1270)$ , and the other  $\rho^0$  acts as a mediator between the photon and the proton.

With this simple picture we determine both the differential cross section and the  $t$  dependence of the integrated cross section over the invariant mass around the resonance with three different models, only vector  $\rho NN$

coupling is considered, both vector and tensor  $\rho NN$  couplings are considered, and the  $\rho$ -Regge propagator is also checked. All these three models can reproduce the experimental data. The agreement with the experimental differential cross sections and the  $t$  dependence is good, thus, providing new support for the  $\rho\rho$  molecular picture of the  $f_2(1270)$ . Furthermore, we calculate also the total cross section of the  $\gamma p \rightarrow p f_2(1270)$  reaction, it is found that the shapes of those three models are different, and our model calculation could be tested by the future experiments at CLAS.

### Acknowledgments

One of us, E. O., wishes to acknowledge support from the Chinese Academy of Science (CAS) in the Program of Visiting Professorship for Senior International Scientists (Grant No. 2013T2J0012). This work is partly supported by the Spanish Ministerio de Economía y Competitividad and European FEDER funds under the contract number FIS2011-28853-C02-01 and FIS2011-28853-C02-02, and the Generalitat Valenciana in the program Prometeo II-2014/068. We acknowledge the support of the European Community-Research Infrastructure Integrating Activity Study of Strongly Interacting Matter (acronym HadronPhysics3, Grant Agreement n. 283286) under the Seventh Framework Programme of EU. This work is also partly supported by the National Natural Science Foundation of China under Grant Nos. 11105126 and 11475227.

- 
- [1] H. Marsiske *et al.* [Crystal Ball Collaboration], Phys. Rev. D **41**, 3324 (1990).  
[2] T. Oest *et al.* [JADE Collaboration], Z. Phys. C **47**, 343 (1990).  
[3] E. Klempt and A. Zaitsev, Phys. Rept. **454**, 1 (2007).  
[4] V. Crede and C. A. Meyer, Prog. Part. Nucl. Phys. **63**, 74 (2009).  
[5] R. Molina, D. Nicmorus and E. Oset, Phys. Rev. D **78**, 114018 (2008).  
[6] M. Bando, T. Kugo, S. Uehara, K. Yamawaki and T. Yanagida, Phys. Rev. Lett. **54**, 1215 (1985).  
[7] M. Bando, T. Kugo and K. Yamawaki, Phys. Rept. **164**, 217 (1988).  
[8] M. Harada and K. Yamawaki, Phys. Rept. **381**, 1 (2003).  
[9] U. G. Meissner, Phys. Rept. **161**, 213 (1988).  
[10] L. S. Geng and E. Oset, Phys. Rev. D **79**, 074009 (2009).  
[11] H. Nagahiro, J. Yamagata-Sekihara, E. Oset, S. Hirenzaki and R. Molina, Phys. Rev. D **79**, 114023 (2009).  
[12] T. Branz, L. S. Geng and E. Oset, Phys. Rev. D **81**, 054037 (2010).  
[13] A. Martinez Torres, L. S. Geng, L. R. Dai, B. X. Sun, E. Oset and B. S. Zou, Phys. Lett. B **680**, 310 (2009).  
[14] L. S. Geng, F. K. Guo, C. Hanhart, R. Molina, E. Oset and B. S. Zou, Eur. Phys. J. A **44**, 305 (2010).  
[15] L. Dai and E. Oset, Eur. Phys. J. A **49**, 130 (2013).  
[16] L. R. Dai, J. J. Xie and E. Oset, arXiv:1503.02463 [hep-ph].  
[17] J. J. Xie and E. Oset, Phys. Rev. D **90**, 094006 (2014).  
[18] R. Aaij *et al.* [LHCb Collaboration], Phys. Rev. D **89**, no. 9, 092006 (2014).  
[19] M. Battaglieri *et al.* [CLAS Collaboration], Phys. Rev. D **80**, 072005 (2009).  
[20] L. Bibrzycki and R. Kaminski, Phys. Rev. D **87**, 114010 (2013).  
[21] A. Ramos and E. Oset, Phys. Lett. B **727**, 287 (2013).  
[22] H. Nagahiro, L. Roca, A. Hosaka and E. Oset, Phys. Rev. D **79**, 014015 (2009).  
[23] R. Machleidt, K. Holinde and C. Elster, Phys. Rept. **149**, 1 (1987).  
[24] J. J. Xie, B. S. Zou and B. C. Liu, Chin. Phys. Lett. **22**, 2215 (2005).  
[25] J. J. Xie and B. S. Zou, Phys. Lett. B **649**, 405 (2007).  
[26] J. J. Xie, B. S. Zou and H. C. Chiang, Phys. Rev. C **77**, 015206 (2008).  
[27] Z. Ouyang, J. J. Xie, B. S. Zou and H. S. Xu, Int. J. Mod. Phys. E **18**, 281 (2009).  
[28] B. Borasoy, P. C. Bruns, U.-G. Meissner and R. Nissler, Phys. Rev. C **72**, 065201 (2005).  
[29] M. Doring, E. Oset and D. Strottman, Phys. Rev. C **73**, 045209 (2006).

- [30] A. V. Barnes, D. J. Mellema, A. V. Tollestrup, R. L. Walker, O. I. Dahl, R. A. Johnson, R. W. Kenney and M. Pripstein, *Phys. Rev. Lett.* **37**, 76 (1976).
- [31] H. Navelet and P. R. Stevens, *Nucl. Phys. B* **118**, 475 (1977).
- [32] M. Guidal, J. M. Laget and M. Vanderhaeghen, *Nucl. Phys. A* **627**, 645 (1997).
- [33] J. M. Laget, *Phys. Rev. C* **72**, 022202 (2005).
- [34] N. I. Kochelev, M. Battaglieri and R. De Vita, *Phys. Rev. C* **80**, 025201 (2009).
- [35] C. R. Ji, R. Kaminski, L. Lesniak, A. Szczepaniak and R. Williams, *Phys. Rev. C* **58**, 1205 (1998).
- [36] K. A. Olive *et al.* [Particle Data Group Collaboration], *Chin. Phys. C* **38**, 090001 (2014).
- [37] H. C. Chiang, E. Oset and L. C. Liu, *Phys. Rev. C* **44**, 738 (1991).
- [38] C. Hanhart, Y. S. Kalashnikova and A. V. Nefediev, *Phys. Rev. D* **81**, 094028 (2010).